

On the role of intergranular carbides on improving the stress corrosion cracking resistance in a cold-worked alloy 600

Zhao Shen ^{a,*}, Junliang Liu ^a, Koji Arioka ^b, Sergio Lozano-Perez ^a

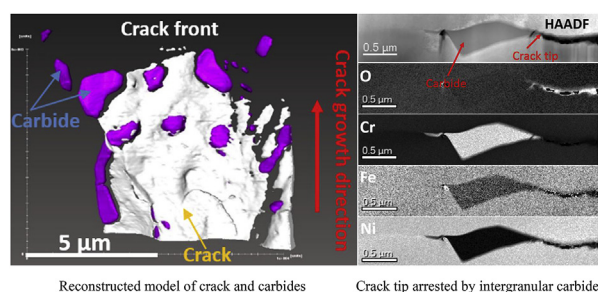
^a Department of Materials, University of Oxford, Parks Road, OX1 3PH, Oxford, UK

^b Institute of Nuclear Safety Systems, Inc. (INSS), 64 Sata, Mihama-cho, Mikata-gun, Fuku, Mihama 919-1205, Japan

HIGHLIGHTS

- Mitigating effect of intergranular carbides on SCC was observed in 3D.
- Cold working-induced preferential deformation around intergranular carbides was observed via TKD.
- Previously reported mechanisms contributing to the mitigating effect were evaluated and discussed.
- A new mechanism based on grain boundary migration inhibition and crack path deviation was proposed.

GRAPHICAL ABSTRACT



ARTICLE INFO

Article history:

Received 13 July 2018

Received in revised form

12 November 2018

Accepted 12 November 2018

Available online 13 November 2018

Keywords:

Alloy 600

Intergranular carbides

Oxidation

3D reconstruction

Transmission electron microscopy

ABSTRACT

The mitigating effect introduced by intergranular Cr carbides on the stress corrosion cracking propagation of a cold-worked Alloy 600 has been firstly examined through high-resolution 3-dimensional (3D) sequential sectioning. High-resolution transmission electron microscope (TEM) and transmission Kikuchi diffraction (TKD) are used to reveal the underlying mechanisms contributing to the mitigating effect. Previously reported mechanisms contributing to the increased stress corrosion cracking resistance are evaluated and discussed. A new mechanism based on grain boundary migration inhibition and crack path deviation is proposed.

© 2019 The Authors. Published by Elsevier B.V. This is an open access article under the CC BY license (<http://creativecommons.org/licenses/by/4.0/>).

Cr carbide precipitation on grain boundaries of Ni-based alloys was reported to decrease the susceptibility to stress corrosion cracking (SCC) in hydrogenated water despite Cr depletion [1–5]. There were mainly two kinds of intergranular Cr carbides ($M_{23}C_6$ and M_7C_3) being reported in literature and the type of the carbide varied with the material composition and the final thermal

treatment [6]. “M” mainly consisted of Cr and a little bit of other metal elements [6]. Although the intergranular carbide mitigating effect has been widely acknowledged, the underlying mechanisms are still under investigation. Considerable work has been conducted to obtain a mechanistic understanding of this phenomenon [1,4,7–11]. Thomas et al. [4] and Was et al. [10] considered that intergranular carbides could facilitate the formation of more protective Cr-rich oxide, which could slow down intergranular oxidation. The authors also found that the carbides could act as oxygen traps, decreasing the grain boundary oxidation rate. Bruemmer

* Corresponding author.

E-mail address: zhao.shen@materials.ox.ac.uk (Z. Shen).

et al. [11] proposed that intergranular carbides could act as effective dislocation sources, which could promote crack tip blunting and thus decrease crack propagation. Arioka et al. [1] believed that the beneficial effect of the intergranular carbides was related to its role on inhibiting grain boundary sliding. More recently, Dugdale et al. [7] found that intergranular carbide deviated the crack from a straight path into a more complex one following the oxide-metal interface around the carbide. The diversion of the crack propagation from the straight path to a curved path can not only increase the total crack path but also decrease the effective stress loaded at the crack tip, resulting in the decline of SCC propagation [10].

Cold-work in alloys was reported to be detrimental to SCC, however, it is inevitable during manufacturing and installation [1,2,12–14]. In the work conducted by Bruemmer et al. [15,16] and Arioka et al. [1], the crack growth rate (CGR) of cold-worked alloys increased with the intergranular carbide coverage. However, the intergranular carbide mitigating effect was still observed by Kunag et al. [17] in cold-worked Alloy 690, although the mechanistic understanding is yet to be established. Thus, a more detailed research is needed to obtain a mechanistic understanding of the intergranular carbide mitigating effect in cold-worked materials.

Recently, Duhamel et al. [18] have shown that 3D sequential sectioning is a very promising technique for investigating the effect of intergranular carbides on the intergranular oxidation. In the current study, high-resolution 3D sequential sectioning was firstly used to directly reveal the 3D relationship between SCC crack and intergranular carbides. Additional characterizations by high-resolution analytical transmission electron microscopy (ATEM) and transmission Kikuchi diffraction (TKD) have also been performed to investigate the chemistry and metallography around the intergranular carbides. With this characterization approach, we have obtained a better understanding of the intergranular carbide mitigating effect on SCC.

The material used in this study was 20% cold-worked Alloy 600 tested under simulated PWR primary water conditions at 360 °C. The SCC tests were conducted by INSS (Japan) using pre-cracked 0.5T compact tension (CT) specimens, extracted in the T-L orientation (crack growth direction parallel to the rolling direction), in an autoclave under a constant load of 30 MPa m^{1/2}. Prior to autoclave testing, the specimen was mill-annealed in air at 930 °C followed by water quenching. More details about the material and the SCC test can be found in Refs. [2,19]. After the autoclave testing the surface containing the crack(s) was ground with SiC paper, followed by polishing with 1-μm diamond suspension. A mirror-finished surface was obtained after 15 min of final treatment with colloidal silica where the SCC cracks and carbides could be easily observed. The intergranular carbide coverage was measured to be around 30%. To examine more crack tips, the surface containing crack tips had been re-polished by the same procedures.

FIB sectioning was carried out on a Zeiss Crossbeam 540 dual beam FIB instrument to obtain 2D SE images. After that all the 2D images were reconstructed using FEI software Avizo Fire 8.1 to acquire a 3D volume. More details can be found in Ref. [20]. FIB plan-view sample preparation technique was used to prepare TEM samples containing intergranular carbide or crack tip in this study. A single beam FEI FIB200 equipped with a static micromanipulator was used for trench milling and in-situ lift-out. A dual beam Zeiss NVision 40 FIB-SEM was subsequently used for thinning the samples to a thickness less than 50 nm. Since FIB milling could introduce significant damage on the sample surface, a final Ga⁺ low energy cleaning (5 kV, 250 pA) was performed on both sides of the foil to minimize the damage. More details can be found in Ref. [19,21]. Once TEM samples were prepared, high-resolution scanning TEM (STEM) and electron energy loss spectroscopy (EELS) were conducted with a JEOL ARM200F (cold-filed emission

gun) operating at 200 kV and equipped with a Quantum Gatan image filter (GIF) spectrometer to reveal the structure and chemical distribution around the carbides or crack tip. To reveal the metallographic information around the intergranular carbides, TKD was performed using a Zeiss Crossbeam 540 FEG-SEM equipped with an Oxford Instrument (OI) EBSD NordlysMax 3 detector. Samples were pre-tilted 20° with respect to horizontal, and the working distance was set to 5 mm. An accelerating voltage of 20 kV and a probe current of 1.5 nA were used. The data was subsequently post-processed by the OI software Channel 5. Image quality and misorientation (MO) maps were calculated automatically by the software. The step size was set to 10 nm. More details about the TKD measurement can be found in [22].

It is necessary to point out that the 3D volume and TEM foils used in this study were prepared from the deepest region of the SCC cracks (same CT specimen), which means we assumed that the cracks were active when they were taken out from the autoclave. However, since crack propagation might not be a continuous process, the cracks used in this study might have been arrested for a while. Since the cracks were prepared from the deepest region, the retardation time could be minimized. As a result, all the conclusions obtained in this study were based on the assumption that the crack fronts were still propagating at the end of the SCC testing.

Eleven crack tips were observed at the deepest region of the SCC cracks. Nine of them were arrested by the intergranular carbides, suggesting that the region with carbides was statistically more resistant to SCC. To understand how the carbides mitigated the SCC crack propagation in 3D, three 3D volumes containing potentially active cracks were prepared. Fig. 1a shows one of the original 3D volumes. Both the carbides and crack can be easily recognized due to different image contrast. The reconstructed 3D volume is shown in Fig. 1b, which shows the crack propagation along a 3D grain boundary plane. The crack was highlighted in white and the carbides were highlighted in purple. In this grain boundary plane, the carbides were discretely distributed. To see more details, only carbides and crack are displayed in Fig. 1c and d. At the crack front region (region 1 and 1'), we found that the crack propagated deeper in the region without carbides but was arrested when it met the carbides, which means the intergranular carbides indeed inhibited the propagation of SCC crack. Another interesting thing that we found is that in the region 2 and 2', some carbides were still connected to both sides of the grain boundary (bridging) when the crack had already propagated into a deeper region. This observation suggests that it is harder for a crack to fracture the connection between the carbide and matrix than a grain boundary. However, the "pinning" or "bridging" effect introduced by the intergranular carbide cannot completely stop the crack propagation because the crack will propagate into a deeper region around it. This might be because the stress could still reach the region ahead of the carbides through plastic deformation or nearby already cracked grain boundary. More details about the "bridging" effect can be found in the supplementary data (see Figs. S1 and S2).

TKD was conducted on a TEM sample containing intergranular carbides. The carbides were identified to be Cr₇C₃ by TKD (see Fig. 2a) and further confirmed by TEM diffraction. In addition, the intergranular carbides were identified as incoherent with the surrounding matrix. The plastic deformation around the carbides was much higher than the part of grain boundary where is free of carbide (see Fig. 2b). The preferential deformation around intergranular carbides was mainly because the hardness of the intergranular carbide was harder than the matrix, which could lead to the preferential accumulation of stress and strain in the matrix around the carbides during the prior 20% cold-work. In a recent study conducted by Lozano-Perez et al. [20], the region suffered a higher extent of deformation (deformation bands) was preferentially

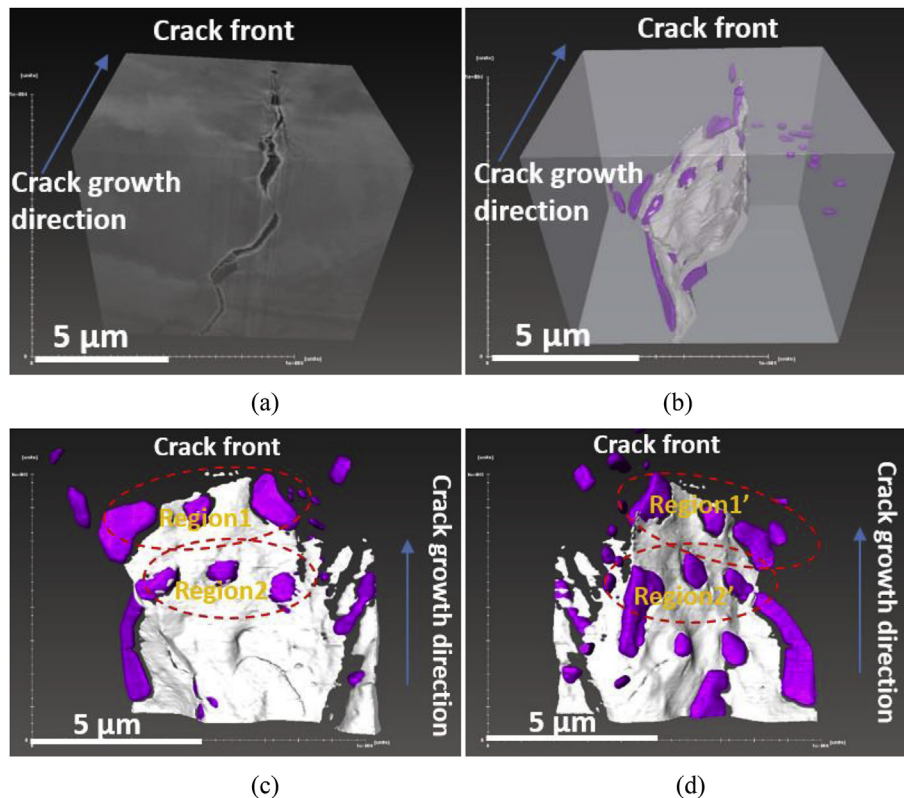


Fig. 1. a) Original 3D volume containing a crack; b) Reconstructed 3D volume using the Avizo Fire software; c) Reconstructed model of crack and carbides (left-view of the crack and carbides in b)); d) Reconstructed model of crack and carbides (right-view of the crack and carbides in b)). The crack is represented in white and the carbides are represented in purple. (For interpretation of the references to colour in this figure legend, the reader is referred to the Web version of this article.)

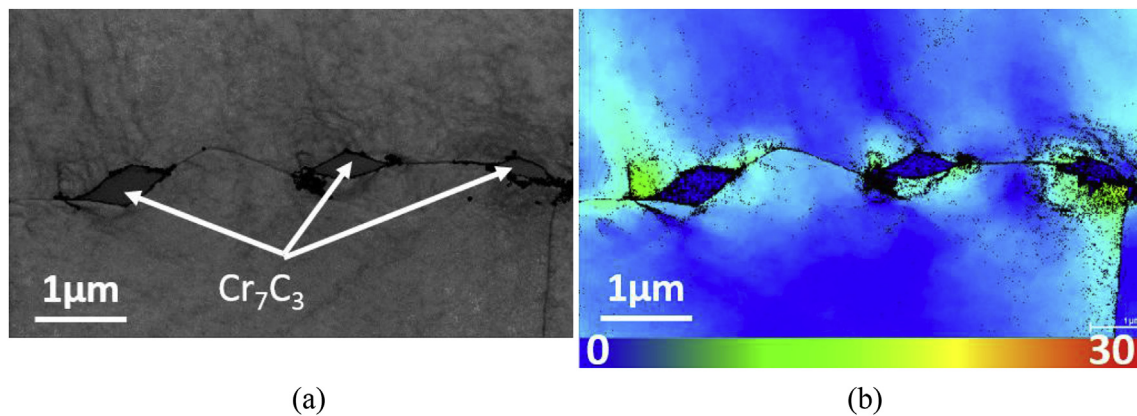


Fig. 2. TKD measurement of the distribution of intergranular Cr carbides. a) Pattern quality map; b) MO map. (Step size = 10 nm).

oxidized. In addition, in a study of the effect of cold work on CGR in austenitic alloys, Terachi et al. [23] revealed that the CGR increased with the extent of cold work. According to these results, the greater extent of plastic deformation around the intergranular carbides might have introduced higher SCC susceptibility, which is in contradiction to what we found in this work (see Fig. 1). As a result, there must be some other factors that could explain their mitigating effect on SCC.

As previously reported in Refs. [4,8–10], Cr carbides can act as oxygen traps and Cr reservoir, facilitating the formation of Cr-rich oxides and thus reducing the intergranular oxidation rate. To verify these hypotheses, ATEM analysis was conducted. Fig. 3 shows the morphology and chemistry around an oxidized intergranular

carbide after the SCC testing. The distance between the carbide and the crack tip was around 2 μm. Although the carbide-matrix interfaces were fully oxidized, the crack only propagated along the interface between the carbide and the Grain 1 (see high angle annular dark field (HAADF) and middle angle annular dark field (MAADF) images in Fig. 3a). The underfocused TEM image (defocus value = −800 nm) in Fig. 3a reveals that although there was no continuous crack in the interface between the carbide and the Grain 2, cavities were observed in this region. To see the elemental distribution in the oxidized interface region, EELS maps and line-scans were acquired. Fig. 3b shows the morphology and elemental distribution around the uncracked interface (Region 1). No Cr enrichment was observed in the oxide surrounding the

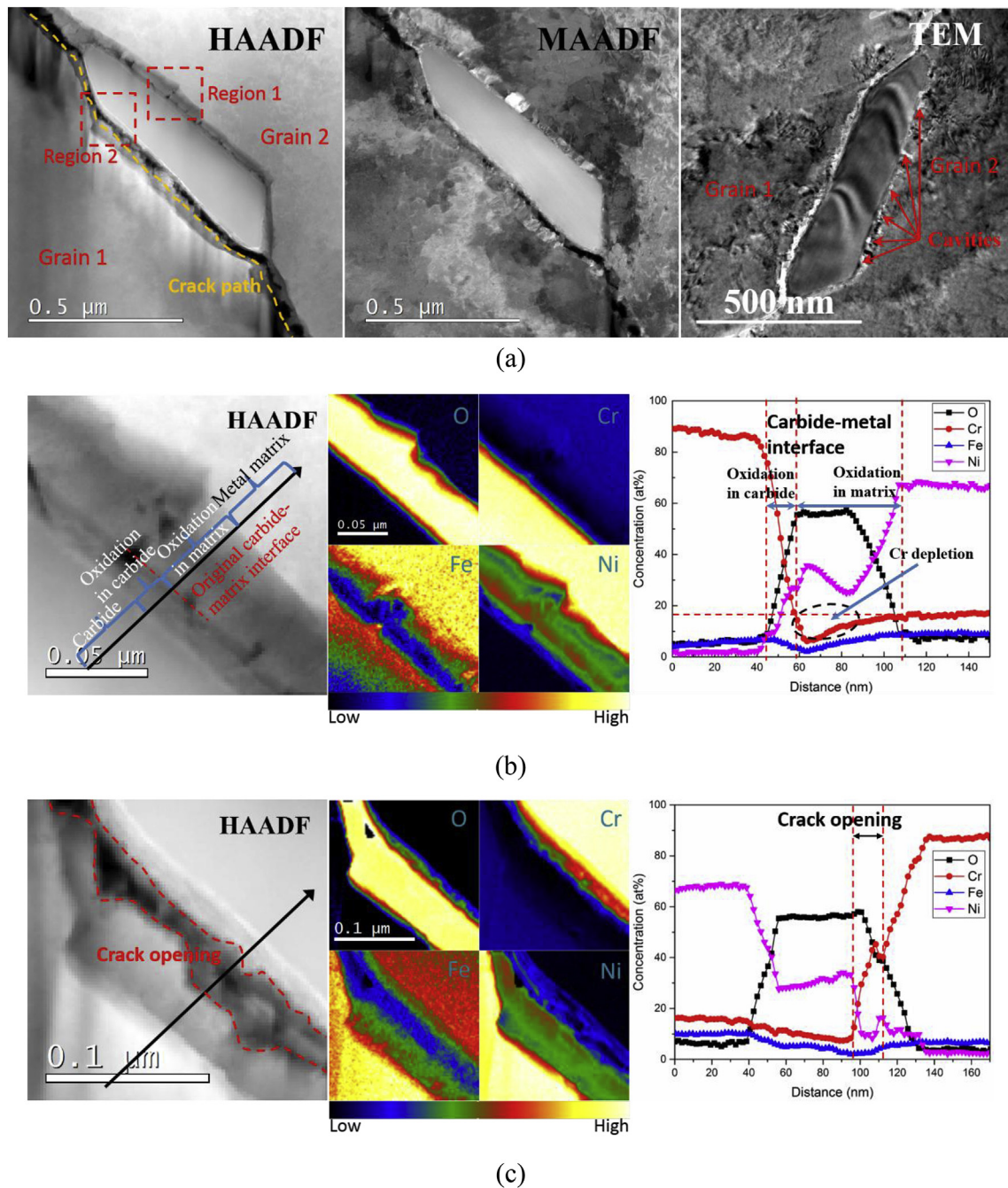


Fig. 3. a) Morphology of intergranular Cr carbide after the SCC propagation; b) morphology and chemistry around the uncracked Carbide-matrix interface; c) morphology and chemistry around the cracked Carbide-matrix interface.

intergranular carbide, which was different from what was reported in Refs. [4,8–10]. In addition, the carbide seemed to be more resistant to oxidation than the matrix since the oxidation depth in the carbide was only a quarter of the oxidation depth in the matrix (in the direction perpendicular to the carbide-metal interface, see the HAADF image in Fig. 3b). The identification of the carbide-metal interface was based on the HAADF image contrast since HAADF image is very sensitive to atomic density. Since the carbide did not preferentially oxidize in this study, it might be not possible to conclude that the carbides could reduce grain boundary oxidation through acting as oxygen traps [4,10]. In addition, no Cr was observed to diffuse into the surrounding oxide. For this reason,

under the test conditions used, we cannot conclude that the carbides could increase SCC resistance through acting as Cr reservoir. EELS mapping and line-scanning were also conducted on the cracked interface (Region 2), as shown in Fig. 3c. A very thin Cr-rich oxide layer (less than 20 nm) was observed on the carbide surface, which was consistent to what was reported in Ref. [8]. Cr was depleted in the matrix surrounding the carbide, which was similar to what was observed in the uncracked interface (region 1). Since this Cr-rich layer on the carbide was very thin, we can detect it only when it was directly exposed. The existence of a Cr-rich oxide layer on the outer surface of the carbide might be the reason why the carbide exhibited higher corrosion resistance than the surrounding

matrix. Given the existence of a Cr-rich oxide layer on the surface of the carbide, it is difficult for the Cr in the carbide to diffuse into the surrounding oxide during the SCC propagation. In contrast, we found the Cr content in the oxide close to the interface was even lower than the region far from the interface (see Fig. 3b). The lower content of Cr in this region might be due to an initial Cr depletion in the alloy surrounding the carbide. Since the thin Cr-rich oxide formed at the carbide-matrix interface can only protect the carbide from further oxidation but not the matrix, it might not appropriate to attribute the increased SCC resistance to the formation of Cr-rich oxide in the region surrounding the intergranular carbides.

TEM analysis around the crack tip region has been proved to be a very promising technique in studying the SCC mechanisms [4,6–9,19,24,25]. According to the results reported in the current work and others [4,8,9,19], a Ni-rich/Cr–Fe depleted zone was always observed ahead of the crack tip. However, the potential role of this zone in SCC was still unclear. Since most of the cracks in this work were arrested by the intergranular carbides, it could be possible to understand the retardation effect introduced by the intergranular carbides through comparing the morphology and chemistry around the crack tips that were arrested by the carbides and those not arrested. Fig. 4a shows the HAADF image and the EELS maps around a potentially active crack tip that was not arrested by a carbide. The typical features around the crack tip were similar to that reported in literature [4,6,9,19,24,25]. The Cr was found to be enriched in the crack tip region, which was believed to be the result of outward diffusion of Cr from the grain boundary ahead of the crack tip, which was found Cr depleted. However, the

Cr-rich oxide at the crack tip was porous [19,26–29], resulting in the formation of an intergranular oxidation zone (IOZ) ahead of the crack tip (see Fig. 4a). Since Cr was depleted in the grain boundary ahead of the crack tip, oxidation could develop faster once the oxidant penetrated into the Cr-depleted zone, accelerating the SCC propagation. According to a recent work conducted by Kuang et al. [28] and Burke et al. [30], the formation of the Cr/Fe-depleted, Ni-enriched zone was the results of grain boundary migration. The work conducted by Langelier et al. [31] revealed that the grain boundary migration could enhance intergranular oxidation along the migrated grain boundary. The relationships between the grain boundary migration and enhanced intergranular oxidation had been discussed in detail in Ref. [19]. As a result, crack propagation along a grain boundary without carbides will result in grain boundary migration ahead of the crack tip, which will then increase the SCC susceptibility through accelerating the intergranular oxidation.

Fig. 4b shows the morphology and chemistry around a crack tip that was arrested by an intergranular carbide. Due to the existence of the carbide, grain boundary composition did not change considerable ahead of the crack tip and no grain boundary migration was observed. As mentioned above, grain boundary migration could enhance intergranular oxidation. As a result, it is sensible to conclude that the decreased SCC susceptibility around the intergranular carbide was because the intergranular carbides could prevent the formation of a Cr-depleted zone or grain boundary migration. Similar phenomenon was also reported in a recent literature that the authors found that the grain boundary migration

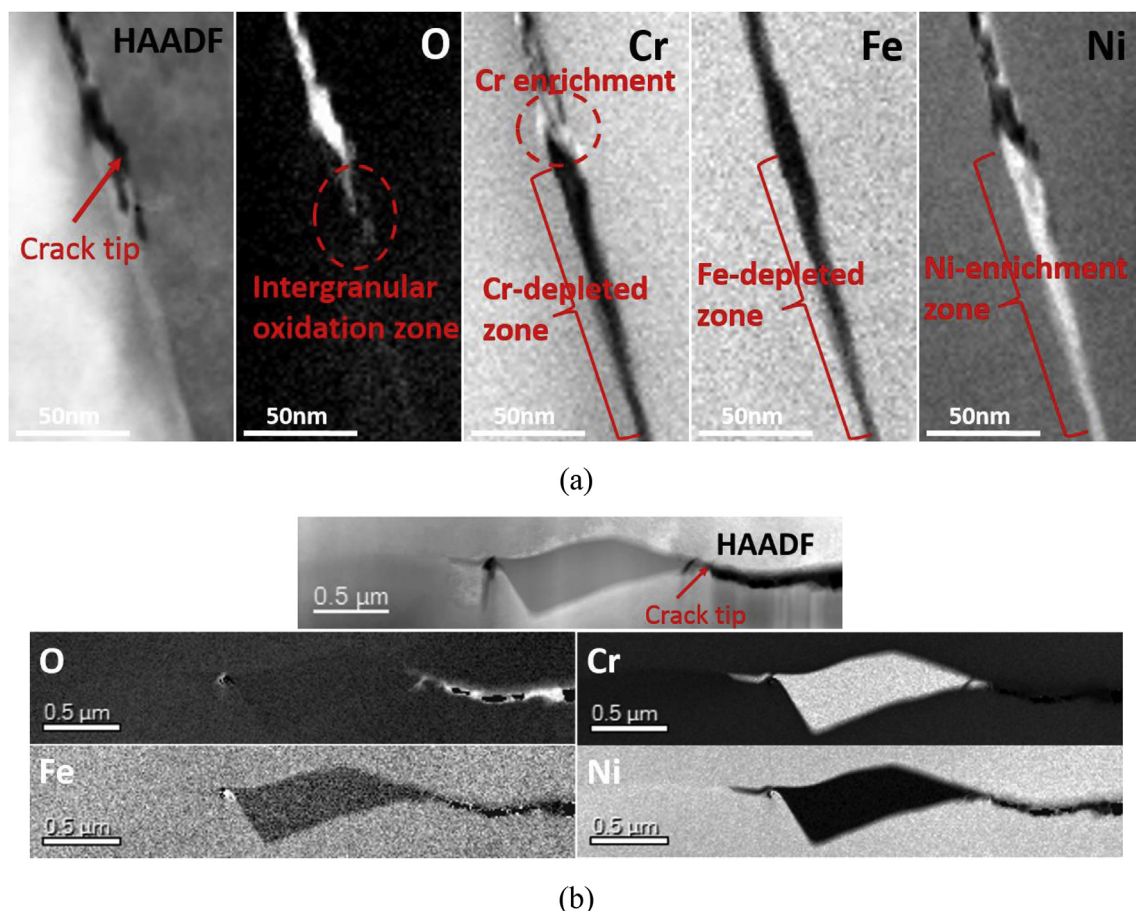


Fig. 4. Morphology and chemistry around a) a crack tip that was not arrested by carbide and b) a crack tip that was arrested by carbide.

along the grain boundary was strongly inhibited by the intergranular carbides [31]. In addition, the existence of intergranular carbide could make the crack propagation deviate from its original path, changing the angle respect the loading direction and increasing the total crack path, resulting in the decrease of CGR. Although it has been proposed that intergranular carbides were supposed to be able to decrease the crack propagation by blunting the crack tip [11], currently no solid experimental evidence exists. Furthermore, crack tip blunting was also not observed in all the crack tips arrested by intergranular carbides in this study. As a result, this hypothesis could also be ruled out for the mitigating effect observed in this study.

According to the work conducted by Bruemmer et al. [15,16], the CGR of 31% cold-worked Alloy 690 increased with the increase of intergranular carbide coverage. The increased SCC susceptibility was attributed to the preferential deformation around the intergranular carbides during the prior cold working, which contradicted to what was observed in the current study. The discrepancy might come from the different level of cold working used in the studies (20% vs. 31%), since the increased SCC susceptibility in the specimen with higher intergranular carbide coverage was only observed in the specimens with high levels of cold working. In addition, different thermal treatment used for different specimens can not only change the intergranular carbide coverage, but also alter other microstructures, such as grain size and Cr concentration at the grain boundaries, which will also affect the SCC susceptibility [1,32]. As a result, the mitigating effect of intergranular carbides on SCC will not disappear if the material only suffers a low level or a middle level of cold working.

It is necessary to point out that the mill-annealed Alloy 600 was rarely used to study the mitigating effect of the intergranular carbides as it is known to have high SCC susceptibility due to its relatively low intergranular carbide coverage compared with thermally-treated Alloy 600 [33–36]. However, the results obtained in this study have clearly revealed the mitigating effect of the intergranular carbides. As a result, the mechanistic understanding obtained in this study is still applicable in the study of mitigating effect of intergranular carbides.

In summary, a more realistic observation of the mitigating effect introduced by intergranular carbides in a cold-worked Alloy 600 was obtained through 3D sequential sectioning, although the prior cold-working has introduced preferential deformation around the intergranular carbides. Under the test conditions, intergranular carbides were rarely oxidized and Cr in the carbides was not observed to diffuse into the surrounding oxide. In addition, crack tip blunting was also not observed around the intergranular carbides. As a result, the increased SCC resistance was neither due to the intergranular carbides acting as oxygen traps or Cr reservoir nor intergranular carbides blunting crack tips, as suggested in literature. However, since the intergranular carbides could locally prevent the grain boundary from migrating, the intergranular oxidation was reduced around them. The decreased SCC susceptibility around intergranular carbides can be then explained as a combination of the incapability of the grain boundary to migrate around the carbide, therefore slowing down intergranular oxidation, and the forced change of propagation direction for the crack around the carbide, requiring higher stresses to break the intergranular oxide.

Acknowledgements

The authors would like to thank INSS (Japan) for providing the sample used in this study and for useful discussions. Zhao Shen is also grateful to China Scholarship Council for providing financial support. The EPSRC (EP/K040375/1, EP/N010868/1 and EP/R009392/1) grants are also acknowledged for funding this research.

Appendix A. Supplementary data

Supplementary data to this article can be found online at <https://doi.org/10.1016/j.jnucmat.2018.11.020>.

References

- [1] K. Arioka, T. Yamada, T. Terachi, G. Chiba, *Corrosion* 62 (2006) 568–575.
- [2] K. Arioka, T. Yamada, T. Miyamoto, M. Aoki, *Corrosion* 70 (2014) 695–707.
- [3] J.L. Hertzberg, G.S. Was, *Metall. Mater. Trans.* 29 (1998) 1035–1046.
- [4] L.E. Thomas, S.M. Bruemmer, *Corrosion* 56 (2000) 572–587.
- [5] P. Berthod, *Oxid. Metals* 68 (2007) 77–96.
- [6] S.M. Bruemmer, G.S. Was, *J. Nucl. Mater.* 216 (1994) 348–363.
- [7] H. Dugdale, D.E. Armstrong, E. Tarleton, S.G. Roberts, S. Lozano-Perez, *Acta Mater.* 61 (2013) 4707–4713.
- [8] M. Sennour, P. Laghoutaris, C. Guerre, R. Molins, *J. Nucl. Mater.* 393 (2009) 254–266.
- [9] Y.S. Lim, H.P. Kim, S.S. Hwang, *J. Nucl. Mater.* 440 (2013) 46–54.
- [10] G.S. Was, K. Lian, *Corrosion* 54 (1998) 675–688.
- [11] S.M. Bruemmer, L.A. Charlot, C.H. Henager, *Corrosion* 44 (1988) 782–788.
- [12] J. Hou, Q.J. Peng, Z.P. Lu, T. Shoji, J.Q. Wang, E.-H. Han, W. Ke, *Corrosion Sci.* 53 (2011) 1137–1142.
- [13] Z. Lu, T. Shoji, S. Yamazaki, K. Ogawa, *Corrosion Sci.* 58 (2012) 211–228.
- [14] E.A. West, G.S. Was, *J. Nucl. Mater.* 441 (2013) 623–632.
- [15] S.M. Bruemmer, M.J. Olszta, M.B. Toloczko, L.E. Thomas, in: *Proceedings of the 15th International Conference on Environmental Degradation of Materials in Nuclear Power Systems—water Reactors*, Springer, Cham, 2011, pp. 301–314.
- [16] M.B. Toloczko, M.J. Olszta, S.M. Bruemmer, in: *Proceedings of the 15th International Conference on Environmental Degradation of Materials in Nuclear Power Systems—water Reactors*, Springer, Cham, 2011, pp. 91–107.
- [17] W. Kuang, G.S. Was, *Corrosion Sci.* 97 (2015) 107–114.
- [18] C. Duhamel, J. Caballero, T. Couvant, J. Crépin, F. Gaslain, C. Guerre, H.T. Le, M. Wehbi, *Oxid. Metals* 88 (2017) 447–457.
- [19] Z. Shen, K. Arioka, S. Lozano-Perez, *Corrosion Sci.* 132 (2018) 244–259.
- [20] S. Lozano-Perez, K. Kruska, I. Iyengar, T. Terachi, T. Yamada, *Corrosion Sci.* 56 (2012) 78–85.
- [21] S. Lozano-Perez, *Micron* 39 (2008) 320–328.
- [22] M. Meisnar, A. Vilalta-Clemente, A. Gholinia, M. Moody, A.J. Wilkinson, N. Huin, S. Lozano-Perez, *Micron* 75 (2015) 1–10.
- [23] T. Terachi, T. Yamada, T. Miyamoto, K. Arioka, *J. Nucl. Mater.* 426 (2012) 59–70.
- [24] M. Meisnar, A. Vilalta-Clemente, M. Moody, K. Arioka, S. Lozano-Perez, *Acta Mater.* 114 (2016) 15–24.
- [25] S. Lozano-Perez, T. Yamada, T. Terachi, M. Schröder, C.A. English, G.D.W. Smith, C.R.M. Grovenor, B.L. Eyre, *Acta Mater.* 57 (2009) 5361–5381.
- [26] K. Kruska, S. Lozano-Perez, D.W. Saxey, T. Terachi, T. Yamada, G.D. Smith, *Corrosion Sci.* 63 (2012) 225–233.
- [27] S.M. Bruemmer, M.J. Olszta, M.B. Toloczko, D.K. Schreiber, *Corrosion Sci.* 131 (2018) 310–323.
- [28] W. Kuang, M. Song, G.S. Was, *Acta Mater.* 151 (2018) 321–333.
- [29] D.K. Schreiber, M.J. Olszta, S.M. Bruemmer, *Scripta Mater.* 89 (2014) 41–44.
- [30] M.G. Burke, G. Bertali, E. Prestat, F. Scenini, S.J. Haigh, *Ultramicroscopy* 176 (2017) 46–51.
- [31] B. Langelier, S.Y. Persaud, A. Korinek, T. Casagrande, R.C. Newman, G.A. Botton, *Acta Mater.* 131 (2017) 280–295.
- [32] T.J. Marrow, L. Babout, A.P. Jivkov, P. Wood, D. Engelberg, N. Stevens, P.J. Withers, R.C. Newman, *J. Nucl. Mater.* 352 (2006) 62–74.
- [33] N. Pessal, G.P. Airey, B.P. Lingenfelter, *Corrosion* 35 (1979) 100–107.
- [34] G. Bertali, F. Scenini, M.G. Burke, *Corrosion Sci.* 114 (2017) 112–122.
- [35] H.A. Domian, R.H. Emanuelson, L.W. Sarver, G.J. Theus, L. Katz, *Corrosion* 33 (1977) 26–38.
- [36] G. Economy, R.J. Jacko, F.W. Pement, *Corrosion* 43 (1987) 727–734.